water

MDPI

*Article*

# Flood Analysis Using HEC-RAS and HEC-HMS: A Case Study of Khazir River (Middle East—Northern Iraq)

**Asaad A. M. AL-Hussein [1,2], Shuhab Khan [3], Kaouther Ncibi [4,*], Noureddine Hamdi [1] and Younes Hamed [3,4]**

1 Department of Water Resources, Higher Institute of Water Sciences and Techniques of Gabes (ISSTEG), University of Gabès, Gabès 6072, Tunisia
2 Department of Sensing and Nanophotonics, Laser and Photonics Research Center, University of Al-Hamdaniya, Nineveh 41006, Iraq
3 Department of Earth and Atmospheric Sciences, Science and Research Building 1, University of Houston, Houston, TX 77204, USA
4 Department of Earth Sciences, Faculty of Sciences of Gafsa, Laboratory for the Application of Materials to the Environment, Water and Energy (LAM3E), University of Gafsa, Gafsa 2112, Tunisia
* Correspondence: nkawther@yahoo.fr

**Abstract:** Floods frequently threaten villages near the Khazir River's floodplains, causing crop losses and threatening residential areas. We used flood-related hydrological software, including WMS and HEC-HMS, to study this issue and determine how to reduce the recurrence of flooding. The software can be used to calculate a hydrograph of torrential flows in a river drainage basin and estimate the volume of torrential water and its flow rates on the Earth's surface. The depth of rain has been evaluated and calculated in the SCS Unit Hydrograph for different return periods of 2, 5, 10, 20, 50, and 100 years. According to our study's findings, the volume of the river's drainage basin floods ranged between 29,680 and 2,229,200 $m^3$, and the maximum flow value ranged between 10.4 and 66.4 $m^3$/sec during various reference periods. To analyze and model the flood risks of the Khazir River, the HEC-RAS model was combined with the HEC-GeoRAS extension in ArcGIS. The floods were the focus of two study periods, 2013 and 2018, and were based on the digital elevation model and river discharge during the floods. According to the classification map of the flood depths, the areas of flood risk varied from low to very low (80.31%), medium (16.03%), and high to very high (3.8%). The analysis of the results revealed that the villages closest to the river's mouth were more affected by the floods than other villages further downstream. HEC-HMS and HEC-RAS have been shown to have a strong correlation in evaluating flood risks and reliably forecasting future floods in the study area.

**Keywords:** Khazir River; floods; Arc GIS; HEC-RAS; HEC-HMS; Iraq

check for updates

**Citation:** AL-Hussein, A.A.M.; Khan, S.; Ncibi, K.; Hamdi, N.; Hamed, Y. Flood Analysis Using HEC-RAS and HEC-HMS: A Case Study of Khazir River (Middle East—Northern Iraq). *Water* **2022**, *14*, 3779. https://doi.org/10.3390/w14223779

Academic Editor: Gilberto Pambianchi

Received: 15 October 2022
Accepted: 17 November 2022
Published: 21 November 2022



## 1. Introduction

Rivers have historically been a significant source of irrigation, hydropower, and drinking water. People who live near rivers, on the other hand, are frequently threatened by flooding because river courses are not always stable in terms of the speed of water flow and the amount of drainage caused by rain [1]. Floods are caused by excessive rainfall, which can take the form of nonstop rain that exceeds the carrying capacity of the riverbed, causing water to flow over the riverbanks and into neighboring areas [2–4]. Many people and their property are at risk, and flooding threatens a large area of fertile land along the riverbank, making it one of nature's worst disasters when it occurs. Floods are regarded as one of the most brutal natural disasters when compared to other disasters [5–7], and the impact on nature is greater than the impact on humans [8,9]. The availability of timely and reliable flood information is critical for reducing post-event disasters in river basins [10]. Flood protection and irrigation management have been two of Mesopotamia's most pressing concerns since the dawn of civilization, during the Sumerians, Akkadians, Babylonians, Assyrians, and Islamic periods. All of these civilizations invested heavily in better organizing and managing their water resources [11–13].

Estimating the volume of runoff caused by rainfall is critical for accurately calculating the quantities needed to store water in reservoirs and determining the likelihood of flooding [14]. Obtaining accurate data and information about flood risks through the interpretation of flood maps is one of the appropriate solutions for preventing and reducing losses caused by floods [15]. Computer models are crucial in the process of developing a hydraulic model and performing a hydraulic analysis of river courses using the (HEC-RAS) program, which is an excellent choice for performing one-dimensional hydraulic calculations in both natural and constructed canal systems [16]. Today, GIS technology is frequently used to model floods or identify flood-prone areas. The HEC-GeoRAS extension employs a set of mathematical equations to calculate river course coefficients based on the speed of river water flow, the amount of drainage, and the rate at which water enters the soil [17]. Numerical flood simulation models are critical tools for quantitative flood assessment, allowing researchers to qualitatively assess the risks and other risks associated with them [18]. Flood modeling is a technical method that can provide precise information on the flood profile, including elements that govern flooding such as precipitation, runoff, and watershed features [19]. Flood maps are intended to provide early warnings to prevent environmental and human harm due to the high wave of the water current and the speed with which it arrives at agricultural land and residential areas, thereby limiting the negative consequences caused by the flood wave after its occurrence [20]. The HEC-HMS Precipitation Runoff Model can simulate and model runoff based on hourly rainfall [21]. All hydraulic calculations that include flow in open water channels must include a study of the features of channel roughness, which is one of the keys to accurately estimating water flow in waterways [22]. Hydraulic modeling is an essential component of any system for predicting river water levels. Accurate and reliable water level predictions aid in the prevention of flood damage and the planning of interventions in the event of major risks [23].

This study was carried out because a number of villages along the river are occasionally flooded. This is especially true in the villages near the river's confluence with the Great Zab River. These villages are in the lower river basin. Thus, the goal of this research was to find appropriate solutions to prevent future floods by analyzing flood water hydrographs for a section of the Khazir River within its lower basin and simulating water levels and side flood plains during floods, as well as to analyze the hydrograph of flood water that flows through the Khazir River drainage basin over different return periods of 2, 5, 10, 20, 50, and 100 years. The hydraulic parameters of the Khazir River were studied to see how the river's course changed as a result of changes in the study region's climate and the amount of precipitation it received. As a result, a section of the Khazir River with a length of 32 km and a cross-section of 60 was chosen.

## 2. Description of the Study Area

The Khazir River originates in Iraqi territory and is formed by the confluence of the Roser and Kafia Rivers. The Khazir River is the main tributary of the Great Zab River, and a number of drainage basins drain into the course of the river. The study area is represented by the lower basin of the river located east of Nineveh Governorate, which is about 37 km away from the city of Mosul. It is located between 43°26′30″ and 43°37′30″ east longitude and 36°10′0″ and 36°21′30″ north latitude. The basin has a surface area of 196.06 $km^2$ and a perimeter of 77.16 km. The highest point within the basin is 413 m, and the lowest point is 237 m. The length of the Khazir River within its drainage basin is 32 km. A network of tree-shaped valleys descends from the high hills towards the Khazir River. Water from these valleys collects in the river's path until it joins the Great Zab River (Figure 1).

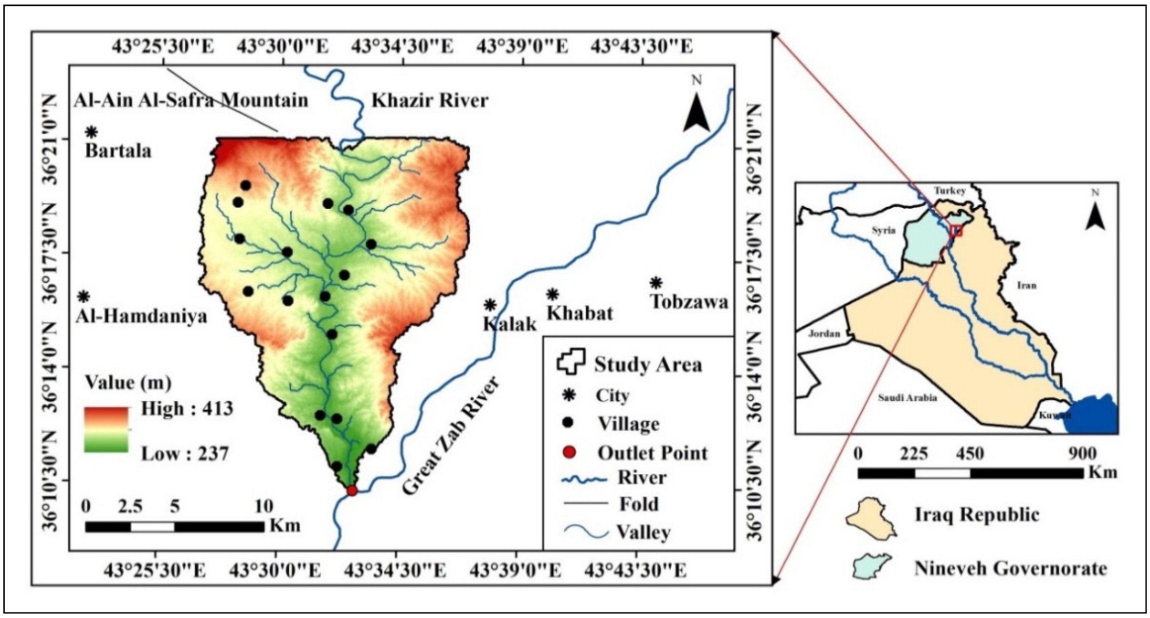


**Figure 1.** Geographical location of the study area.

The climate of the study area is similar to that of the Mediterranean basin, with rain in the winter, and high temperatures with no rain at all in the summer. The climatic zones established by Al-Sahhaf in 1976 serve as the foundation for the mountain climate. The analysis of other climatic elements (temperature, wind, relative humidity, evaporation), as well as the development of the volume of torrential rains causing them, plays a significant and influential role in hydrological work on the surface of the earth. Rainfall storms create water flows after saturation of the land with water, causing water torrents within river drainage basins after hours of rain that may take one, two, or three days, and the development of the volume of torrential rains causes them.

Surface water runoff has a direct relationship with the amount of precipitation that occurs. In turn, this causes the production of water torrents that vary in size, speed, and direction in which they move across the surface area they touch. The volume of surface water runoff increases in proportion to the amount of precipitation that falls. The present study relied on climatic data from the NASA site for the years encompassing the period 1989–2021 because there was no climate monitoring station close to the research site. Although the amount of precipitation that occurs in a particular year fluctuates from year to year, on average there are 260.35 mm of precipitation throughout the year. November marks the start of precipitation, which lasts until May. The greatest monthly average temperatures ranged from 16.54 to 46.64 °C, and the lowest monthly average temperatures ranged from 0 to 22.81 °C, with an annual average temperature of 21.49 °C. Between summer and winter, the temperatures vary dramatically.

## 3. Materials and Methods

### *3.1. Data Collection*

To model and simulate Khazir River Basin floods, all relevant data (Table 1) were used, including climatic data received from NASA and spanning a period of daily, monthly, and yearly rainfall and temperature readings from 1989 to 2021. A digital elevation model with a spatial accuracy of 14 m was used to identify the basin's slope and its impact on water flow, as well as a topographic map at a scale of 1:250,000, maps of land and soil uses at a scale of 1:50,000, a modern satellite image for the year 2022 and the daily discharge of the Khazir River, with the construction of the measurement station on the river's course beginning in 2004.

**Table 1.** Information and data collected about the Khazir River Basin.

| No. | Data | Information | Resources |
|---|---|---|---|
| 1 | Rainfall | Data for the years 1989–2021 | NASA |
| 2 | Temperature | Data for the years 1989–2021 | NASA |
| 3 | DEM | STRM, 14 m resolution | USGS www.usgs.gov (accessed on 25 May 2022) |
| 4 | Topographic map | Paper map, 1:250,000 scale | Iraqi Armed Forces Military area |
| 5 | Land use image | LULC, 10 m resolution | Sentinel-2 |
| 6 | Soil map | Hydrologic Soil Groups | USDA, 2005 |
| 7 | Landsat 8 image | 30 m resolution | USGS www.usgs.gov (accessed on 25 May 2022) |
| 8 | Discharges and depths of the Khazir River | Data for the years 2004–2021 | Duhok Irrigation Directorate/Iraq |

When simulating floods on rivers with the HEC-RAS software, two types of data are used: hydraulic data and engineering data. These are required to run the simulation successfully. HEC-RAS employs river flow data and a digital elevation model with a spatial accuracy of fourteen meters. It uses the Manning special value of 0.035 for the river banks within the model (Steady Flow Data) and bases its findings on the values determined by the scientist Chow [24]. The Manning roughness modulus is essential in hydraulic analysis because it indicates the interaction between river flow and topography, which influences water current speed [25].

Data from the Dohuk Irrigation Directorate's Asmawa station for the period 2004–2021, corresponding to the date the station was established on the riverbank, were used in the flood simulation procedure (Table S1, Supplementary Material). The river's expenditures were high during the winter months, particularly in January, and dramatically decreased during the summer and fall months, particularly in August, according to data collected by the station. These data were consistent with the amount of precipitation that fell in the research area during the time period specified. The current study modeled floods for the years 2013 and 2018, because the study region was more impacted by floods during this period due to high river flows.

## *3.2. Methodology*

A descriptive and analytical method was used to investigate the hydraulics of the Khazir River course, with modern techniques in interpretation and analysis based on Arc GIS 10.8 software after adding the HEC-GeoRAS software extension. Next, the flood simulation data were exported from Arc GIS 10.8 into HEC-RAS 5.0.3 software, which was designed by the United States Army Hydrological Engineers for river, port, and other facility management [26,27]. The hydrological model known as HEC-HMS, which is included in the WMS software, was used to estimate the magnitude of the torrents as well as their flow rates within the drainage basin.

### 3.2.1. Hyfran Plus

Hyfran Plus is one of the statistical analysis programs used to compute the maximum depth of rainfall for different return periods, including 2, 5, 10, 20, 50, and 100 years. It is also used to compute the intensity and intensity curves of rainfall (IDF Curve), providing a precise calculation of the amount of precipitation that fell on the drainage basin. One of the most important factors that helps with accurate calculation of the torrents created by those rains is considered to be the most trustworthy basis for figuring out water statistics and the likelihood of future torrents [28]. Further employing the Normal Method Equation in statistical analysis [29]:

$$f(x) = \frac{1}{x\sigma\sqrt{2\pi}} exp\left[-\frac{[Inx-\mu]_0^2}{2\sigma^2}\right] \quad (1)$$

where:

*f(x)*: Number of observations
$\sigma$: Standard deviation
$\mu$: Mean

### 3.2.2. Watershed Modeling System (WMS)

This is a sophisticated computer program that offers an advanced graphical interface for the development and use of a large number of hydrological and hydraulic mathematical models. It is easier, faster, and more accurate than GIS applications [30].

### 3.2.3. HEC-GeoRAS

HEC-GeoRAS is an expansion of Arc GIS software, which was first developed through a research and development partnership between the Hydrological Engineering Center (HEC) and ESRI and is still being developed utilizing R&D funds [27]. It is a set of GIS tools developed particularly for analyzing geographic data using the Hydrological Engineering River Analysis System (HEC-RAS). Through this extension, the engineering data of the river's course may be constructed and transferred to a program called HEC-RAS that enables the development of a map showing the flood and the speed of the water current inside the drainage basin.

### 3.2.4. Hydrologic Model HEC-HMS

This model was created by the Center for Hydrological Engineering and the US Army Corps of Engineers. It has been extensively utilized in numerous hydrological research projects and is intended to simulate rainfall-runoff processes in a wide range of geographic regions, including floods, water supplies, local and large river basins, and urban and natural watershed runoff [31]. There are four main parts of this model that work together to calculate the volume of runoff: direct runoff, base flow, and channel flow [32]. The working of this model with WMS software is described in Figure 2.

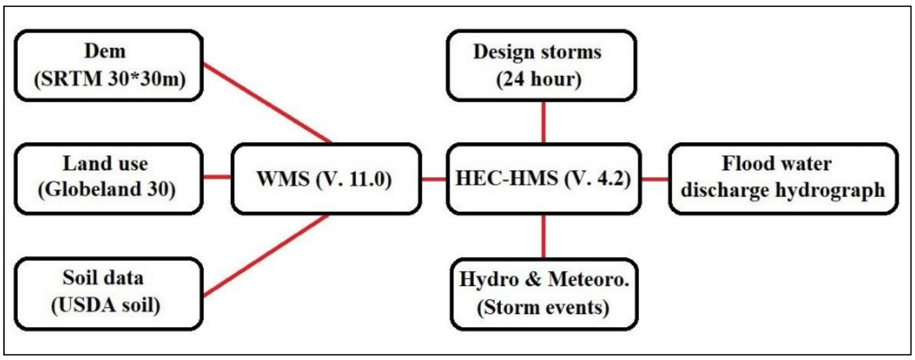


**Figure 2.** Flowchart for HEC-HMS methodology.

### 3.2.5. Hydrodynamic Model HEC-RAS

The HEC-RAS software is the river analysis system of the Center for Hydrological Engineers, and it is a hydraulic computer program that creates hydraulic component models. It is specialized in modeling and simulating water through natural waterways such as rivers and industrial courses such as canals and drains, and the software can calculate the movement of sediments and chemical pollutants in a stream [33]. This program computes the water levels and velocity in rivers and builds one- or two-dimensional models to simulate the movement of water, in either a steady state or an unsteady state.

### 3.2.6. Calculation of Hydraulic Parameters

The hydraulic characteristics of the Khazir River were calculated using a steady one-dimensional flow model using Equations (1) and (2). The conventional step approach is used to calculate the water surface height and the energy degree line for two neighboring cross-sections [34].

$$Y_1 + \frac{a1\ V1^2}{2g} + Z_1 = Y_2 + \frac{a2\ V2^2}{2g} + Z_2 + he \quad (2)$$

where:

Z1, Z2: Elevation of the main channel inverts (m)
Y1, Y2: Depths of water at cross section (m)
V1, V2: Average velocities (total discharge/total flow area) (m/s)
a1, a2: Velocity weighting coefficients
g: Gravitational acceleration ($m/s^2$)
he: Energy head loss (m)

$$he = L * S_f + C\left[\frac{a1\ v1^2}{2g} + \frac{a2\ v2^2}{2g}\right] \quad (3)$$

where:

L: Discharge weighted reach length (m)
$\overline{s_f}$: Representative friction slope between two adjacent sections
C: Contraction or expansion loss coefficient

### 3.2.7. Boundary Conditions

The boundary conditions are needed to determine the depth of the water both upstream and downstream [35]. Where the value of water discharge in cubic meters and the value of water depth along the studied section are entered in meters, and the high daily expenditures of the Khazir River in the study area for the two years 2013 and 2018, amounted to 372.15 $m^3$/sec and 506.16 $m^3$/sec, respectively, were relied on, because these values caused flooding that harmed the riverbanks, nearby residential and agricultural regions.

### 3.2.8. Hydraulic Modeling Application

In order to generate hydrological and hydraulic models of the course of the Khazir River using the HEC-RAS model, the following three key stages must be followed:

1. Using the Arc GIS program and the HEC-GeoRAS extension, along with a digital elevation model and a recent satellite image of the research area, the following riverine hydraulic coefficients are generated (Figure 3):
    a. The main channel.
    b. The left and right banks.
    c. The left and right flow paths.
    d. Cross sections.
2. Working within the HEC-RAS software, this phase includes the processing stage (Figure 4), to outline the flood plain and simulate the flow of water in riverbeds after exporting the data received from the Arc GIS software. Geometric data, including cross-sections, stable flow data, and their surrounding conditions, are entered using

a one-dimensional Steady Flow Data model, which predicts the water surface and velocity along the river well [36]. That is after entering Manning's coefficient of cross-sectional materials of banks, which was 0.035, as well as the depth of the water for the cross-sections and the volume of water drainage, and then performing hydraulic calculations for these data.

3. This step includes the post-processing stage, which entails exporting the data and results obtained from the HEC-RAS software to the Arc GIS software as they appear in the workspace and consist of a polygon connecting the ends of the river's cross-sections. Using the water surface generation command, all of the HEC-RAS-created partitions will be recognized, and the flood zone will border both banks of the river. The user can create a flood map and determine the depth of the water, its surface area, and its volume inside the riverbed by using the raster's floodplain delineation command.

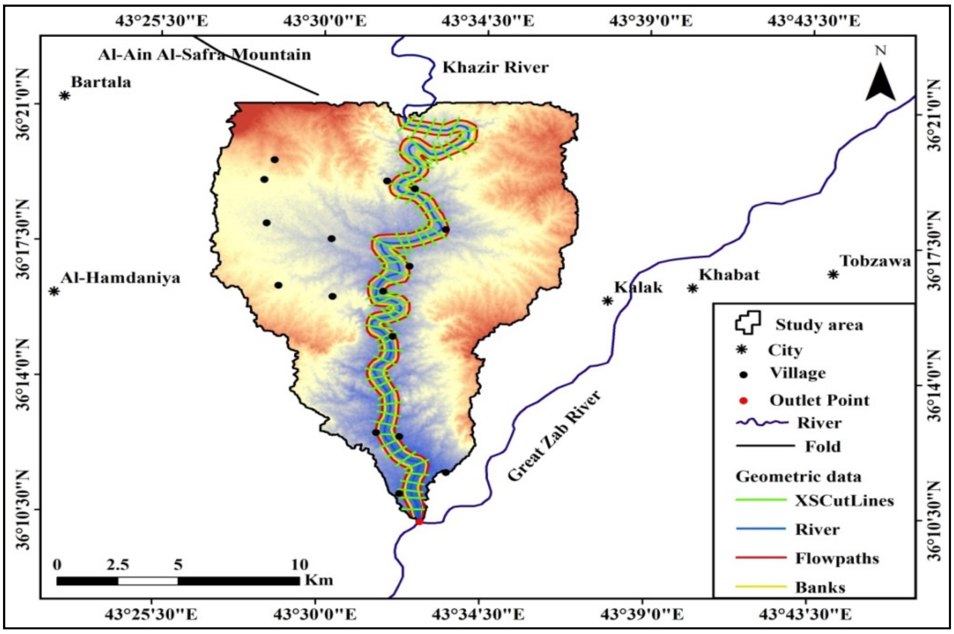


**Figure 3.** Geometric data of Khazir River.

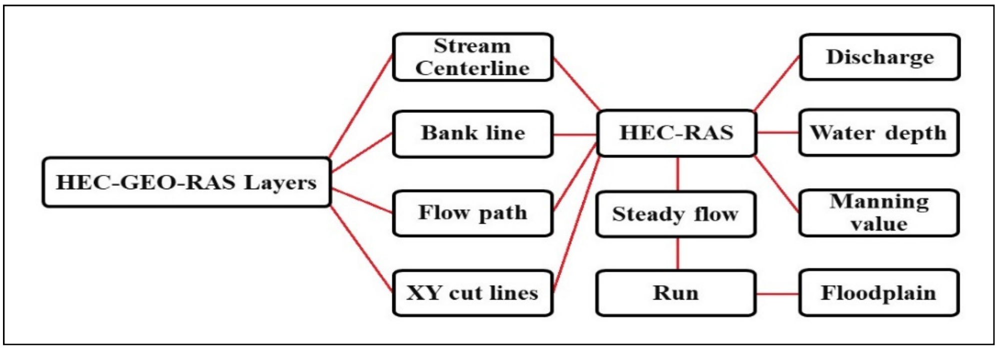


**Figure 4.** Flowchart for HEC-RAS methodology.

## 4. Results and Discussion

### *4.1. Hydrology Setting*

#### 4.1.1. Analysis of Rainfall in the Khazir River Basin

Precipitation analysis is critical for effectively estimating flood risk and forecasting the likelihood of future flooding in the drainage basin because it provides the most reliable data on which to base flood predictions. We determined the rainfall depth for different frequency intervals of 2, 5, 10, 20, 50, and 100 years, as well as for the period 1989–2021, after obtaining the maximum annual rainfall quantities for each year (Table 2). Using the statistical analysis software Hyfran Plus, the depth of rain influencing the Khazir River drainage basin at various recurrent times was determined (Table 3).

**Table 2.** The maximum amounts of rainfall in the station of the study area.

| Year | Maximum Daily Rainfall (mm) | Year | Maximum Daily Rainfall (mm) | Year | Maximum Daily Rainfall (mm) |
|---|---|---|---|---|---|
| 1989 | 43.67 | 2000 | 18.30 | 2011 | 44.49 |
| 1990 | 21.74 | 2001 | 9.42 | 2012 | 19.38 |
| 1991 | 19.54 | 2002 | 15.19 | 2013 | 31.99 |
| 1992 | 19.65 | 2003 | 12.24 | 2014 | 21.01 |
| 1993 | 25.37 | 2004 | 18.52 | 2015 | 23.41 |
| 1994 | 18.53 | 2005 | 15.39 | 2016 | 32.41 |
| 1995 | 10.33 | 2006 | 40.42 | 2017 | 20.51 |
| 1996 | 17.65 | 2007 | 15.09 | 2018 | 29.58 |
| 1997 | 14.28 | 2008 | 18.58 | 2019 | 37.92 |
| 1998 | 17.13 | 2009 | 20.08 | 2020 | 52.87 |
| 1999 | 14.36 | 2010 | 24.25 | 2021 | 21.17 |

**Table 3.** Precipitation depths (mm) as a function of return periods.

| Statistical Distribution | Design Rainfall Depth for Different Recurring Times | | | | | |
|---|---|---|---|---|---|---|
| | Years | | | | | |
| | **2** | **5** | **10** | **20** | **50** | **100** |
| Normal | 23.2 | 32 | 36.6 | 40.4 | 44.7 | 50.2 |

Statistics for the research region's station, including the number of years, maximum and minimum daily precipitation amounts, mean, standard deviation, and other fundamental data (Table 4). By choosing the curve whose rain points were closest to the storm curve, the normal approach was chosen as one of the ideal probability distributions for rain depth (Figure 5).

**Table 4.** Summary of rainfall for the study area station.

| Number of Year | 33 |
|---|---|
| Minimum | 9.42 |
| Maximum | 52.9 |
| Average | 23.2 |
| Standard deviation | 10.5 |
| Median | 19.6 |
| Coefficient of variation (Cv) | 0.453 |
| Skewness coefficient (Cs) | 1.29 |
| Kurtosis coefficient (Ck) | 3.55 |

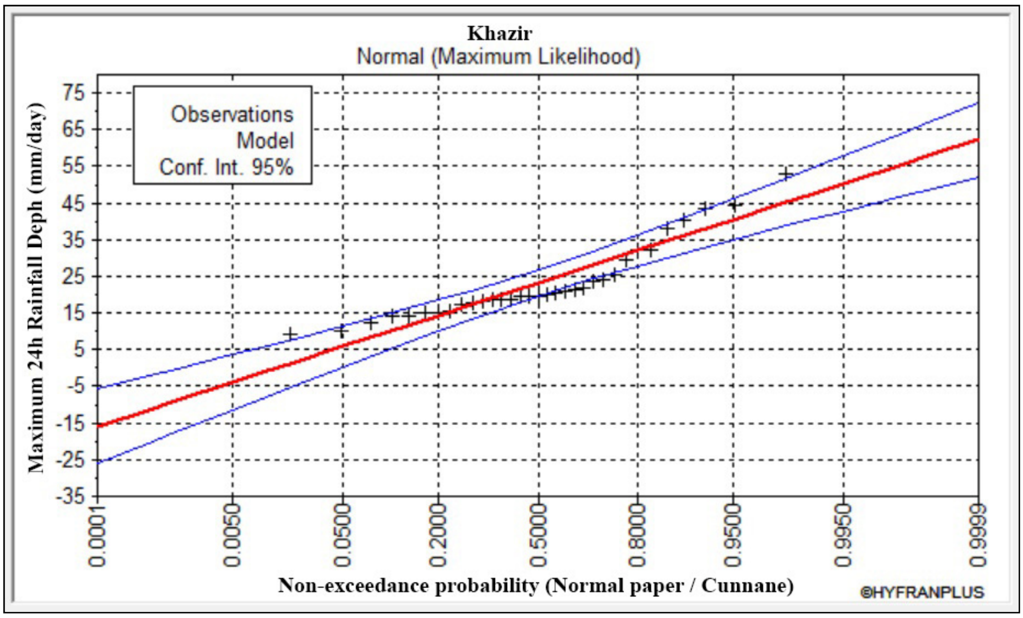


**Figure 5.** Curve values (intensity, duration, frequency) for the study station.

IDF curves were generated from daily rainfall data due to the lack of climate data regarding the intensity of rainfall in the research area. Using Bell's Ratios, the rainfall value was calculated for the time intervals of 10, 20, 30 min, 1, 2, 3, 6, and 12 h as a percentage of the previously predicted daily rain value for the various recurring times, as shown in Table 5.

**Table 5.** Percentage of rainfall value at different periods (Bell's Ratios).

| Time (Min) | 10 | 20 | 30 | 60 | 120 | 180 | 360 | 720 | 1440 |
|---|---|---|---|---|---|---|---|---|---|
| Bell Average | 0.2 | 0.279 | 0.343 | 0.435 | 0.565 | 0.626 | 0.75 | 0.877 | 1 |

The following equation can be used to calculate the values of the curves (density, duration, and frequency) shown in Table 6, and these values can then be graphically represented (Figure 6).

**Table 6.** Curve values (intensity, duration, frequency) for different return periods to the study station.

| Return Periods | Time (Min) | | | | | | | | |
|---|---|---|---|---|---|---|---|---|---|
| | 10 | 20 | 30 | 60 | 120 | 180 | 360 | 720 | 1440 |
| 100 | 68.701 | 47.904 | 39.258 | 24.894 | 16.166 | 11.941 | 7.153 | 4.182 | 2.384 |
| 50 | 61.174 | 42.656 | 34.957 | 22.166 | 14.395 | 10.633 | 6.369 | 3.724 | 2.123 |
| 20 | 55.289 | 38.552 | 31.594 | 20.034 | 13.010 | 9.610 | 5.757 | 3.365 | 1.919 |
| 10 | 50.088 | 34.926 | 28.622 | 18.149 | 11.787 | 8.706 | 5.215 | 3.049 | 1.738 |
| 5 | 43.793 | 30.536 | 25.025 | 15.868 | 10.305 | 7.612 | 4.560 | 2.666 | 1.520 |
| 2 | 31.750 | 22.139 | 18.143 | 11.504 | 7.471 | 5.518 | 3.306 | 1.940 | 1.102 |

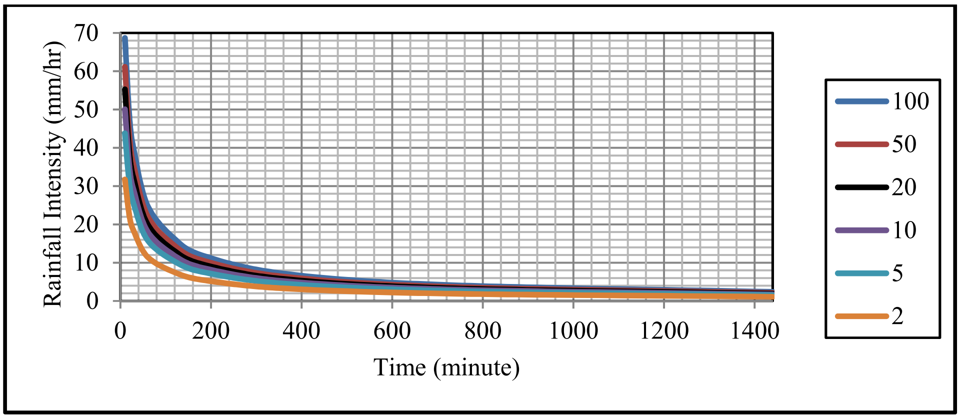


**Figure 6.** Curve values (intensity, duration, and frequency) for the study station.

$$I = \frac{(XT * B)}{(T/60)} \tag{4}$$

where:

I: Rainfall Intensity (mm/hr)
XT: 1.14 (HYFRAN XT)
B: Bell Ratio as per Table 6
T: Duration (min)

The rain depth values given in Table 7 and shown in Figure 7, can be determined using the equation:

**Table 7.** Depth of rainfall for different return periods of the study station.

| Return Periods | Time (Min) | | | | | | | | |
|---|---|---|---|---|---|---|---|---|---|
| | **10** | **20** | **30** | **60** | **120** | **180** | **360** | **720** | **1440** |
| 100 | 11.450 | 15.968 | 19.629 | 24.894 | 32.332 | 35.823 | 42.918 | 50.184 | 57.216 |
| 50 | 10.195 | 14.218 | 17.478 | 22.166 | 28.790 | 31.899 | 38.214 | 44.688 | 50.952 |
| 20 | 9.214 | 12.850 | 15.797 | 20.034 | 26.020 | 28.830 | 34.542 | 40.380 | 46.056 |
| 10 | 8.348 | 11.642 | 14.311 | 18.149 | 23.574 | 26.118 | 31.290 | 36.588 | 41.712 |
| 5 | 7.298 | 10.178 | 12.512 | 15.868 | 20.610 | 22.836 | 27.360 | 31.992 | 36.480 |
| 2 | 5.291 | 7.379 | 9.071 | 11.504 | 14.942 | 16.554 | 19.836 | 23.280 | 26.448 |

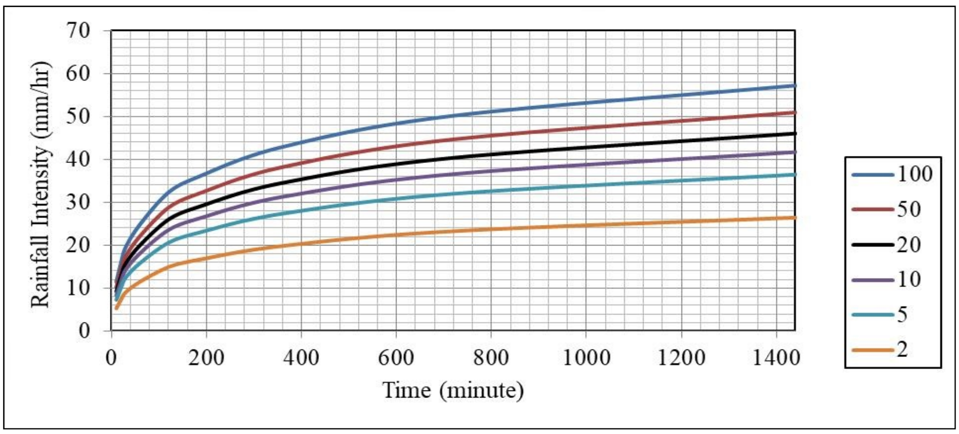


**Figure 7.** Curve values (depth, duration, and frequency) for the study station.

$$D = I * T/60 \quad (5)$$

where:

D: Rainfall depth (mm)
I: Rainfall intensity (mm/hr)
T: Duration (min)

In addition to the aforementioned, it can be argued that rainfall depths and return durations in the Khazir River drainage basin have an effective hydrological value that is influenced by land use. Its effectiveness increases when the surface receiving this rainfall is impermeable, such as in urban and rocky areas, providing a great opportunity for a high runoff response by converting the majority of the rain precipitation into surface running water and increasing the likelihood of flooding.

#### 4.1.2. Floodwater Characteristics Analysis of the Khazir River Basin

The WMS software was used to determine the characteristics of the Khazir River drainage basin, and the HEC-HMS software was used to analyze the torrential waters due to its ability to calculate the hydrographic curve in multiple ways depending on the area of the drainage basin, using natural or artificial methods [37]. It is sophisticated computer software that models and simulates the relationship between precipitation and surface runoff in water drainage basins. The most important outputs are the computations of groundwater discharge and seepage, water movement in streams, the number of losses, total leaching, residual rainfall, and direct runoff [32,38]. The HEC-HMS software gives reliable data and is recommended above other programs when it comes to analyzing the features of torrents [39].

We used a design storm with a 24 h duration, the SCS TYPE II distribution type, and the SCS technique to calculate the concentration-time, delay, and hydrograph curve number (Table 8) for the different recurrence periods of 2, 5, 10, 20, 50, and 100 years. The hydrograph of the torrential waters in the Khazir River drainage basin was analyzed, and the results showed that the volume of the discharge ranged between 29,680 and 2,229,200 $m^3$ during the various return periods and that the maximum flow of the peak discharge was between 10.4 and 66.4 $m^3/s$ during the various return periods. The features of the Khazir River's torrential flows are shown in Table 9 and Figures 8 and 9 using the WMS and HEC-HMS software.

**Table 8.** Some hydrological characteristics of the Khazir River drainage basin.

| Lag Time (h) | Concentration Time (h) | Curve Number | Hydrologic Soil Groups | |
|---|---|---|---|---|
| 7.16 | 7.12 | 84.37 | B | Sandy soil with average depth and moderate infiltration after moistening the soil |
| | | | D | Clay soils having a very slow infiltration rate (high runoff potential) when thoroughly wet |

**Table 9.** Characteristics of the flood water of the Khazir River Basin for different return periods.

| Periods (Years) | 2 | 5 | 10 | 20 | 50 | 100 |
|---|---|---|---|---|---|---|
| Precipitation volume (mm) | 23.2 | 32.0 | 36.6 | 40.4 | 44.7 | 50.20 |
| Loss volume (mm) | 20.07 | 24.67 | 26.64 | 28.10 | 29.58 | 31.26 |
| Excess volume (mm) | 3.13 | 7.33 | 9.96 | 12.30 | 15.12 | 18.94 |
| Discharge volume (1000 $m^3$) | 296.8 | 784.4 | 1102.9 | 1392.5 | 1745.1 | 2229.2 |
| Peak discharge ($m^3$/sec) | 10.4 | 24.6 | 33.8 | 42.3 | 52.5 | 66.4 |

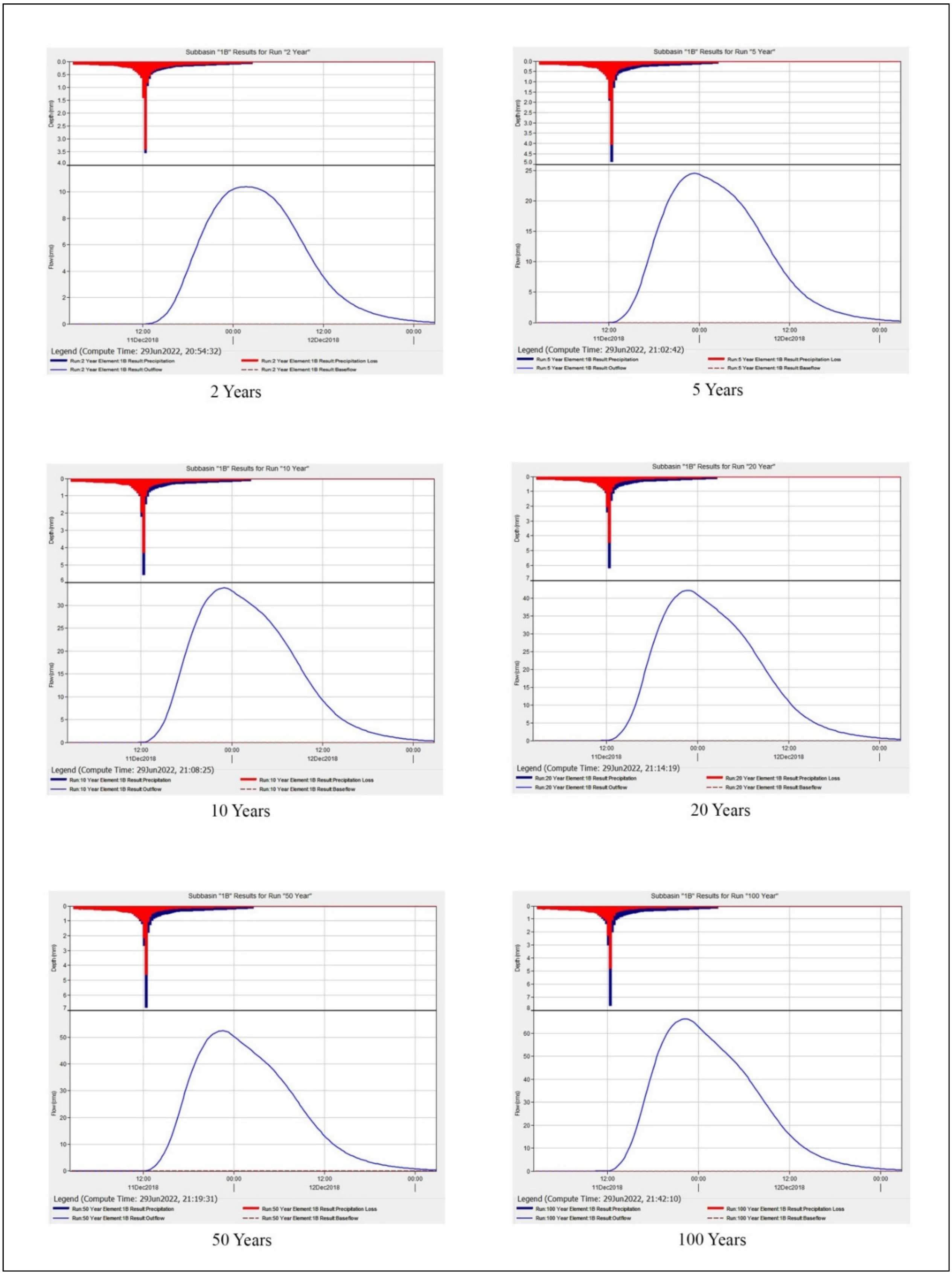


**Figure 8.** Hydrograph of the flood water of the Khazir River Basin for return periods.

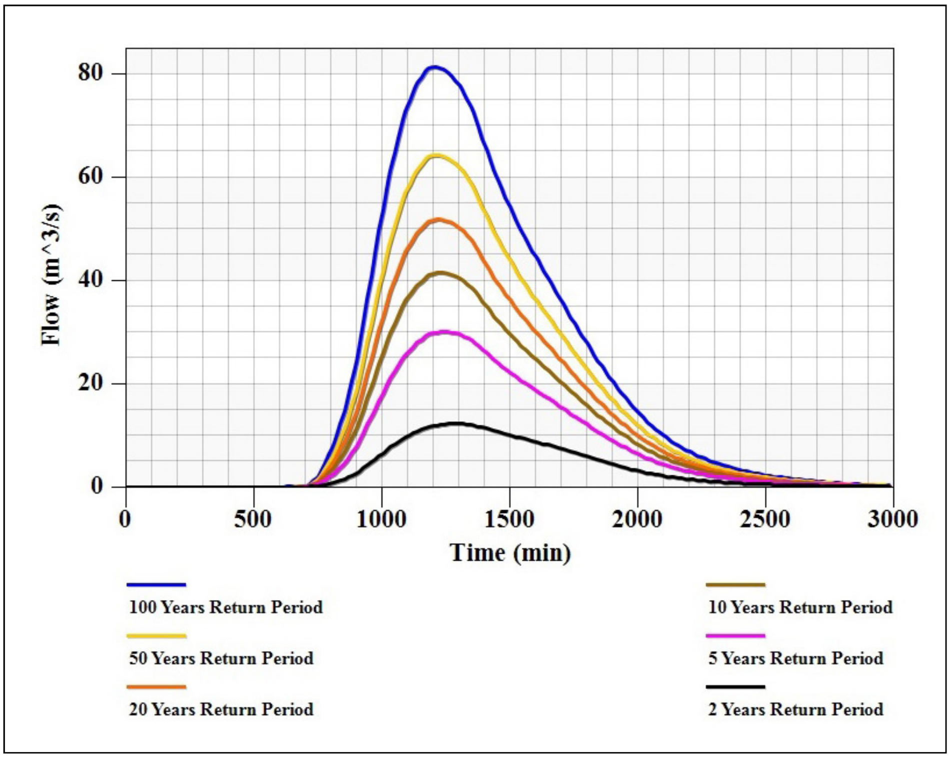


**Figure 9.** Hydrograph of the flood water of the Khazir River Basin for different return periods.

### *4.2. Simulation of Floods in the Khazir River Basin*

Over the two years 2013 and 2018, a flood simulation model for the Khazir River Basin was developed because the research region was more vulnerable to flooding due to high river flows at the time (Table 10). There was a strong correlation between the amount of precipitation that fell on the basin and the river discharge during the study period. A three-day rainstorm was responsible for the flooding in each case, as the confluence of wet days caused water runoff and flooding. The HEC-RAS software was used to independently simulate and estimate flood risk for each year. For each discharge, a flood map and a speed map were created, and it was discovered that as the amount of discharge to the river increased, so did the flood regions, flood depths, and water velocity (Table 11). Additionally, the degree of flooding along the watercourse varied from one area to another. Residential areas and agricultural fields near the river's mouth were more vulnerable to the threat of flooding than places farther away from the estuary, and the risk of flooding was categorized in accordance with [40,41] and based on the flood's depth (Table 12).

**Table 10.** Hydrological characteristics of the river during the study period.

| Year | Day | Precipitation (mm) | Discharge ($m^3/s$) | Level of Water (m) |
|---|---|---|---|---|
| 2013 | 27 January 2013 | 12.35 | 105.74 | 2.25 |
| | 28 January 2013 | 23.12 | 173.9 | 2.95 |
| | 29 January 2013 | 31.99 | 372.15 | 5.5 |
| 2018 | 29 November 2018 | 0.33 | 10.16 | 0.47 |
| | 30 November 2018 | 11.95 | 48.8 | 1.44 |
| | 1 December 2018 | 29.58 | 506.16 | 5 |

**Table 11.** Flood water characteristics of the river during the study period.

| Year | Mean Depth (m) | Total Flood Volume ($m^3$) | Area of Buildings Affected by the Flood ($m^2$) | Area of Agricultural Land Affected by the Flood ($m^2$) | Total Flood Area ($m^2$) |
|---|---|---|---|---|---|
| 2013 | 2.7 | 30,207.97 | 786 | 10,402.14 | 11,188.14 |
| 2018 | 2.87 | 33,893.55 | 903.046 | 10,906.55 | 11,809.60 |

**Table 12.** Flood risk classification.

| Flood | No. | Depths (m) | Area ($m^2$) | Area (%) | Flood Risk Classification |
|---|---|---|---|---|---|
| 2013 | 1 | 0–1.35 | 5095.6 | 45.54 | Very low |
| | 2 | 1.36–2.79 | 3941.36 | 35.23 | Low |
| | 3 | 2.80–4.36 | 1750.11 | 15.65 | Medium |
| | 4 | 4.37–6.43 | 324.956 | 2.90 | High |
| | 5 | 6.44–10.80 | 76.111 | 0.68 | Very high |
| 2018 | 1 | 0–1.49 | 5168.80 | 43.77 | Very low |
| | 2 | 1.50–2.99 | 4260.80 | 36.08 | Low |
| | 3 | 3.0–4.66 | 1937.20 | 16.40 | Medium |
| | 4 | 4.67–6.81 | 357.60 | 3.03 | High |
| | 5 | 6.82–11.20 | 85.20 | 0.72 | Very high |

#### 4.2.1. Case 1: 2013 Flood

The process of creating a flood plain map model and the depth, velocity, and spatial distribution of flood waters depended on entering the Khazir River's maximum flow rate, which in 2013 was 372.15 $m^3/s$ following three days of intense rain that resulted in the formation of water torrents within the river and its basin. The total area of the flood was 11,188.14 $m^2$, the surface area of the agricultural fields near the riverbank that were flooded was 10,402.14 $m^2$, the surface area of the residential structures that were flooded was 786 $m^2$, and the volume of flood water was 30,207.97 $m^3$.

According to the flood map, the speed of the water current varies along the river's path, fluctuating between 0 and 3.4 m/s, and the speed of the water current increases as the river's channel meanders more (Figure 10b). While Figure 10a shows that flood levels vary along the river's course, it also shows that depths vary along the river's length. Whereas the high depths were concentrated in cross-sections that resembled the letter (V) and were located in areas with topography and steep slope, the low depths were concentrated in cross-sections that resembled the letter (U) and represented areas with minimal slope and low topography. And as we approach the basin's mouth, the flood depths decrease (Figure 11).

#### 4.2.2. Case 2: 2018 Flood

When modeling and simulating floods in 2018, the same methods and programs as in 2013 were used, with the exception of a change in the value of the river discharge, which was 506.16 $m^3/s$. Where the study area was exposed to heavy rains for three consecutive days, which led to an increase in the water level within the water channel, and then with the continued rains led to the flow of water towards the two banks of the river, and the flood water covered large areas of land near the riverbed and reached 11,809.6 $m^2$, an increase of 621.46 $m^2$ over the flood of 2013. The flood water inundated agricultural grounds covering an area of 10,906.554 $m^2$, while residential structures were flooded covering an area of 903.046 $m^2$, and the volume of flood water reached 33,893.552 $m^3$.

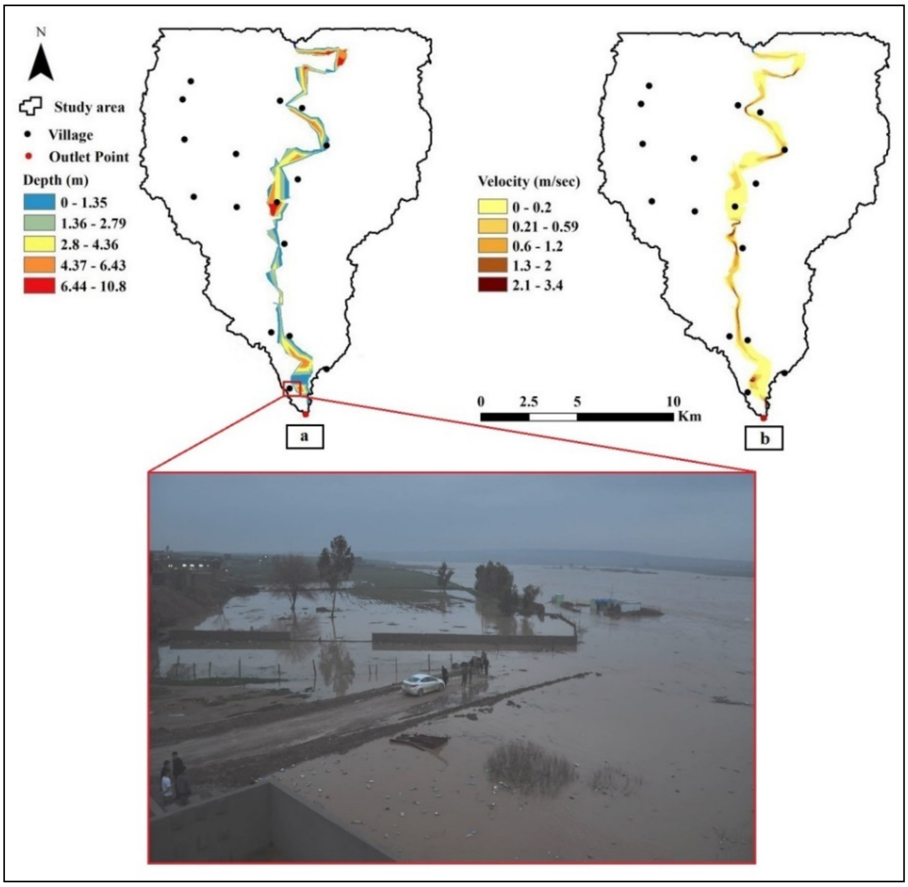


**Figure 10.** (**a**) Floodplain depths map; (**b**) Water current velocity map.

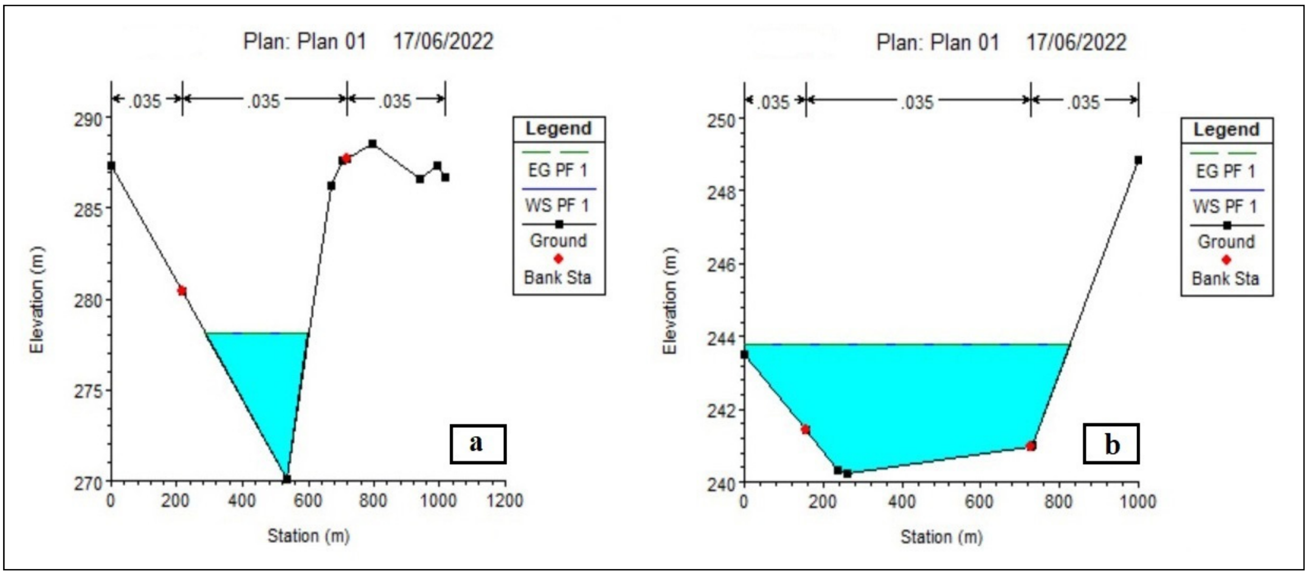


**Figure 11.** River cross sections for 2013 (**a**) upstream and (**b**) downstream.

The high depths are concentrated in cross-sections that look like the letter (V) and are found in areas with topography and steep slopes, whereas the low depths are concentrated in cross-sections that look like the letter (U) and are found in areas with little slope and flat terrain. The flood gets shallower as we get closer to the basin's mouth (Figure 12). The speed of the water current varies along the course of the river, and the cause of this variation is the unevenness of the river within the research area, as the speed ranged between 0 and 3.7 m/s (Figure 13b). Figure 13a depicts the variation in the riverbed flood depths. A rise in the water level within the river channel is observed, as is an increase in the water discharge value for 2018 when compared to 2013.

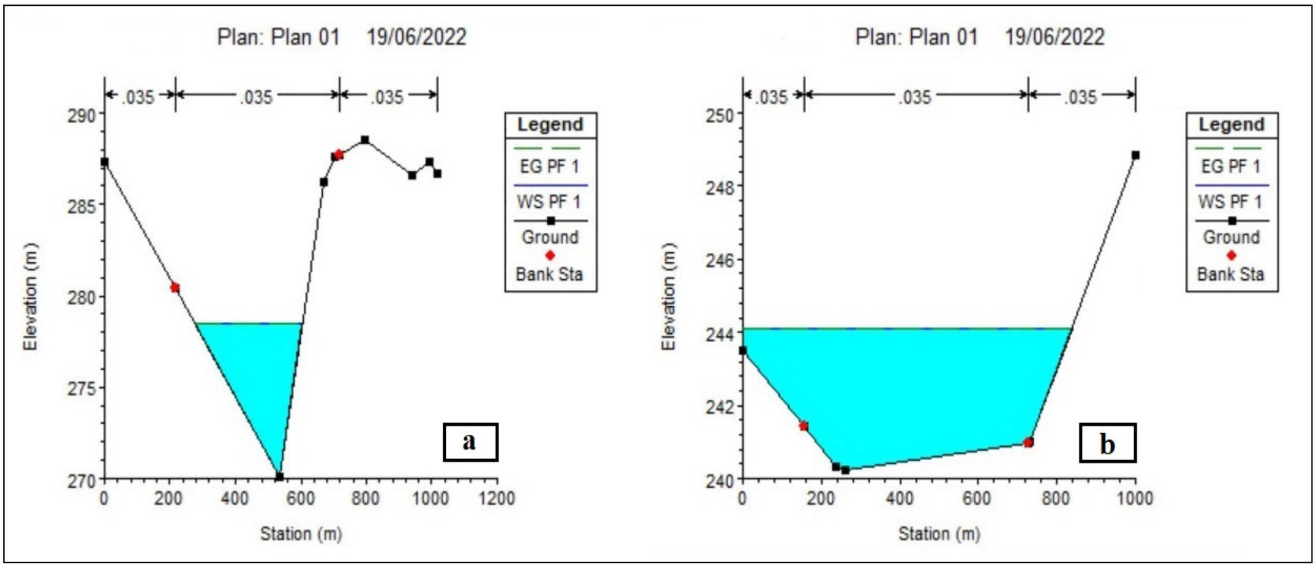


**Figure 12.** River cross-sections for 2018 (**a**) upstream and (**b**) downstream.

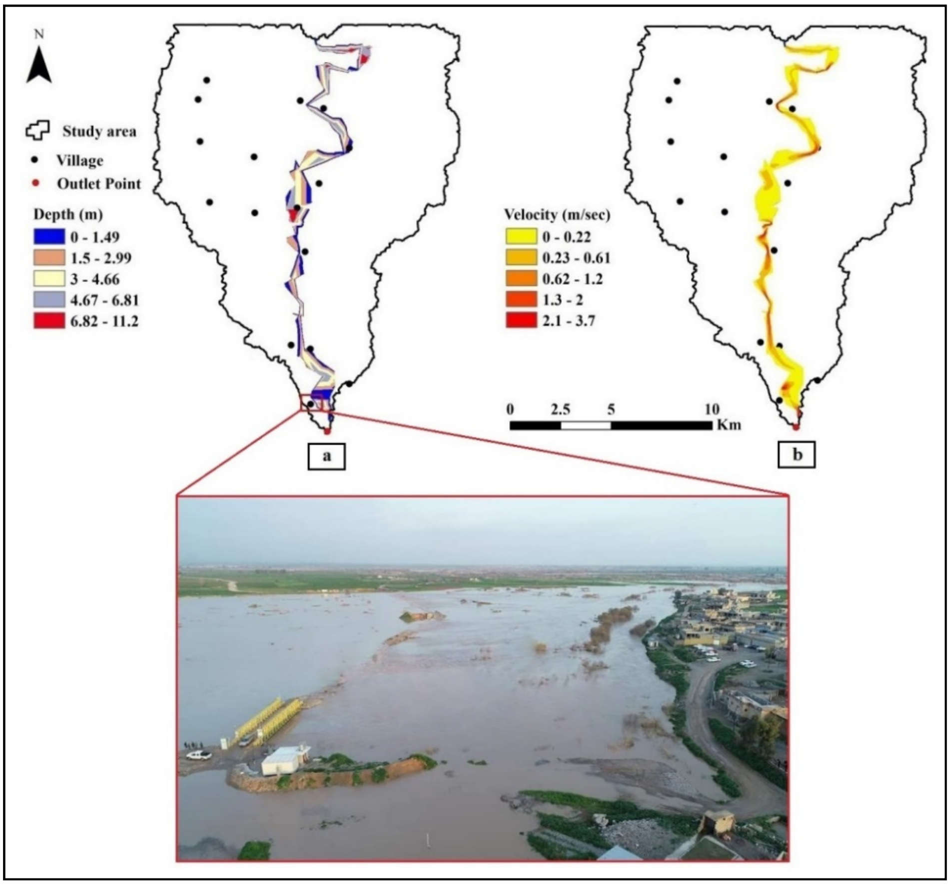


**Figure 13.** (**a**) Floodplain depths map; (**b**) Water current velocity map.

The flood area of the research region was determined by natural features of the river drainage basin, which was a significant and effective factor. The digital elevation model (DEM) revealed that the low regions of the basin are more prone to flooding than the high regions. The land use map displayed the impact of flooding on agricultural lands versus residential areas. The increase in surface water runoff volume has been significantly influenced by the quality of the soil in the basin. The length of the rainstorm had a significant impact on the occurrence of the flood because the longer the rainstorm, the greater the risk of flooding. The convergence of rainy days caused flooding due to an increase in riverbed water levels, and thus an increase in the speed and volume of water discharge. All of the above information was derived from an analysis of the results obtained from the software and models used in the research.

## 5. Conclusions and Recommendations

The Khazir River is one of the important rivers that feed the Great Zab River in Nineveh Governorate, and the course of this river within its lower basin is occasionally exposed to a rise in water levels due to heavy rainfall and an increase in discharge rates, resulting in the flow of water towards neighboring lands close to the course, particularly those with low topography and little slope. It was discovered that the depths of rain falling on the river drainage basin and for different return periods of 2, 5, 10, 20, 50, and 100 years have an effective hydrological value that is influenced by the type of land use and that this value increases when the surfaces receiving these rains are impermeable. This increases the chance of floods by channeling the majority of precipitation to surface runoff, resulting in a strong runoff response. Using the hydrological model HEC-HMS, the analysis of the hydrograph of the torrential waters of the river drainage basin revealed that the volume of the torrents ranged between 29,680 and 2,229,200 $m^3$ and the maximum flow value of the torrents ranged between 10.4 and 66.4 $m^3/s$ during the different return periods, and 70.60% of the rainfall that falls on the drainage basin filters into the ground, while 29.40% runs on the surface of the land through a network of valleys descending from high places towards the river's path.

Floods were simulated using the HEC-RAS software and Steady Flow Data during the winter seasons of 2013 and 2018, and the simulation process provided useful information on the occurrence of floods in the research region, such as the flood's speed and depth, as well as the impacted areas. The investigation's findings revealed a variation in flood danger along the Khazir River's course, with flood risk regions ranging from low to very low (80.31%), medium (16.03%), and high to very high (3.8%), according to categorization. This discrepancy was influenced by the geography of the land, the amount of water drainage, and the shape and depth of the river stream. The settlements at the entrance of the basin were badly impacted by the magnitude of the flood as a result of the rise in the amount of water entering from the feeding areas and the decrease in ground level. The river's flow velocity varied over its course, ranging from 0 to 3.55 m/s, with convex river bends and short cross sections showing an increase in velocity. The study suggests routine upkeep of the riverbed by removing sediments carried by the water from the basin's valleys as well as all bushes, herbs, and weeds that are widely dispersed at the river's bottom and along its banks in order to observe the most amount of running water possible during the river's increased flow during the wet seasons. Further, work to build dirt barriers on the riverbanks to stop water from flowing towards agricultural land and residential structures, while advising people not to live near the riverbed and to produce lands in high locations distant from the fear of floods. Additionally, the report recommends utilizing the hydrological model HEC-HMS in a study on flood risk reduction and the management of infrastructure facilities.

**Supplementary Materials:** The following supporting information can be downloaded at: https://www.mdpi.com/article/10.3390/w14223779/s1, Table S1: Discharge data of the Khazir River for the period 2004–2021.

**Author Contributions:** A.A.M.A.-H. performed field activities and wrote the original draft of the paper; S.K. conceived and designed the study; A.A.M.A.-H. collected data and data curation with the supervision of N.H. and Y.H.; K.N. visualized and revised the manuscript. All the authors have read and agreed to the published version of the manuscript. All authors have read and agreed to the published version of the manuscript.

**Funding:** This research received no external funding.

**Institutional Review Board Statement:** Not applicable.

**Informed Consent Statement:** Not applicable.

**Data Availability Statement:** I have included all data in my main manuscript file.

**Acknowledgments:** We would like to express our gratitude to the Ministry of Irrigation in the Kurdistan region of Iraq for providing us with hydrological data on the Khazir River. We also thank the residents of the flood-prone villages for their hospitality and for providing us with a set of necessary and critical information about the dates of the floods in the research area and the effects they caused. The authors express their grateful thanks to the reviewers who generously contributed their time and expertise to improve the quality of the manuscript.

**Conflicts of Interest:** The present paper is an original work and all the authors declare that they have no conflicts of interest. The authors confirm that they are not associated with or involved in any profitable organization or company that has any financial interest.

## References

1. Azhar, H.; Mohammed, S.; Mohammed, L.A. Simulation of Floods in Delhi Segment of River Yamuna Using HEC-RAS. *Am. J. Water Resour.* **2018**, *6*, 162–168.
2. Singh, S.K.; Kanga, S.; Đurin, B.; Kranjčić, N.; Chaurasia, R.; Markovinović, D. Flood risk modeling using HEC-RAS and geospatial techniques. *E-ZBORNIK Electron. Collect. Pap. Fac. Civ. Eng.* **2021**, *11*, 20–36. [CrossRef]
3. Hamed, Y.; Hadji, R.; Redhaounia, B.; Zighmi, K.; Bâali, F.; El Gayar, A. Climate impact on surface and groundwater in North Africa: A global synthesis of findings and recommendations. *Euro-Mediterr. J. Environ. Integr.* **2018**, *3*, 1–15. [CrossRef]
4. Hamed, Y.; Hadji, R.; Ncibi, K.; Hamad, A.; Ben Saad, A.; Melki, A.; Khelifi, F. Modelling of potential groundwater artificial recharge in the transboundary Algero-Tunisian Basin (Tebessa-Gafsa): The application of stable isotopes and hydroinformatics tools. *Irrig. Drain.* **2022**, *71*, 137–156. [CrossRef]
5. Ashley, S.T.; Ashley, W.S. Flood fatalities in the United States. *J. Appl. Meteorol. Climatol.* **2008**, *47*, 805–818. [CrossRef]
6. Seyedeh, S.; Thamer, A.; Mahmud, A.; Majid, K.; Amir, S. Integrated Modelling for Flood Hazard Mapping Using Watershed Modelling System. *Am. J. Eng. Appl. Sci.* **2008**, *1*, 149–156.
7. Stefanidis, S.; Stathis, D. Assessment of flood hazard based on natural and anthropogenic factors using analytic hierarchy process (AHP). *Nat. Hazards* **2013**, *68*, 569–585. [CrossRef]
8. IRFC. *World Disasters Report*; International Federation of Red Cross and Red Crescent Societies: Paris, France; Imprimerie Chirat: Lyon, France, 2003.
9. ARDC. *Natural Disaster Data Book (an Analytical Review)*; Asia Disaster Reduction Center: Kobe, Japan, 2009; p. 23.
10. Ali, S.; Cheema, M.J.M.; Waqas, M.M.; Waseem, M.; Leta, M.K.; Qamar, M.U.; Awan, U.K.; Bilal, M.; Rahman, M.H.U. Flood Mitigation in the Transboundary Chenab River Basin: A Basin-Wise Approach from Flood Forecasting to Management. *Remote Sens.* **2021**, *13*, 3916. [CrossRef]
11. El Gayar, A.; Hamed, Y. Climate change and water resources management in Arab countries. In Proceedings of the Euro-Mediterranean Conference for Environmental Integration, Sousse, Tunisia, 20–25 November 2017; pp. 89–91.
12. Abdullah, M.; Al-Ansari, N.; Adamo, N.; Sissakian, V.K.; Laue, J. Floods and Flood Protection in Mesopotamia. *J. Earth Sci. Geotech. Eng.* **2020**, *10*, 155–173.
13. Besser, H.; Hamed, Y. Environmental impacts of land management on the sustainability of natural resources in Oriental Erg Tunisia, North Africa. *Environ. Dev. Sustain.* **2021**, *23*, 11677–11705. [CrossRef]
14. Hamdan, A.N.A.; Almuktar, S.; Scholz, M. Rainfall-Runoff Modeling Using the HEC-HMS Model for the Al-Adhaim River Catchment, Northern Iraq. *Hydrology* **2021**, *8*, 58. [CrossRef]
15. Zin, W.W.; Kawasaki, A.; Takeuchi, W.; San, Z.M.L.T.; Htun, K.Z.; Aye, T.H.; Win, S. Flood hazard assessment of Bago River Basin, Myanmar. *J. Disaster Res.* **2018**, *13*, 14–21.
16. Ameera, M.A. Hydraulic Model Development using HEC-RAS and Determination of Manning Roughness Value for Shatt Al-Rumaith. *Muthanna J. Eng. Technol.* **2016**, *4*, 9–13.
17. Marina, I.; Oana, E.C. *The Use Of HEC–RAS Modeling in Flood Risk Analysis*; Carol I, No. 20; Alexandru Ioan Cuza" University, Faculty of Geography: Iași, Romania, 2015; pp. 315–322. Available online: https://www.academia.edu/17596342/ (accessed on 29 April 2021).

18. Tsakiris, G.D. Flood risk assessment: Concepts, modelling, applications. *Nat. Hazards Earth Syst. Sci.* **2014**, *14*, 1361–1369. [CrossRef]
19. Hakim, F.A.; Akhtar, A.; Sultan, B.; Shabir. A One Dimensional Steady Flow Analysis Using HEC-RAS: A Case of River Jhelum, Jammu, and Kashmir. *Eur. Sci. J.* **2016**, *12*, 340–350. [CrossRef]
20. Kamaledin, E.B.; Basim, H.K.; Ghassan, K.K. Inundation Map Development by Using Hec-Ras Hydraulic Simulation Modeling From Rosaries to Khartoum Cities. *Indian J. Res.* **2014**, *3*, 58–62.
21. CEIWR-HEC; HEC-HMS. *Hydrological Modeling System: Application Guide*; US Army Corps of Engineers Hydrologic Engineering Center: Davis, CA, USA, 2017; pp. 3.1–3.19.
22. Lahsaini, M.; Tabyaoui, H. Mono Dimensional Hydraulic Modeling by HEC RAS, Application on L'oued Aggay (City of Sefrou). *Eur. Sci. J. Ed.* **2018**, *14*, 110–121. [CrossRef]
23. Mohammed, A.B.; Pascal, M.; François, A. Uncertainty Analysis of a 1D River Hydraulic Model with Adaptive Calibration. *J. Water* **2020**, *12*, 1–24.
24. Chow, V.T. *Open Channel Hydraulics*; McGraw-Hill: New York, NY, USA, 1959.
25. Bennani, O.; Tramblay, Y.; El Mehdi, S.M.; Gascoin, S.; Leone, F. Flood Hazard Mapping Using Two Digital Elevation Models: Application in a Semi-Arid Environment of Morocco. *Eur. Sci. J.* **2019**, *15*, 338–359.
26. Merwade, V. *Creating SCS Curve Number Grid using HEC-GeoHMS*; School of Civil Engineering, Purdue University: West Lafayette, IN, USA, 2012; pp. 101–114.
27. US Army Corps of Engineers, Hydrologic Engineering Center. *HEC-RAS, River Analysis System-Hydraulic User's Manual*; US Army Corps of Engineers, Hydrologic Engineering Center: St. Davis, CA, USA, 2016; pp. 1–538.
28. Abdelkarim, A. The effect of spatial changes of urban growth and land uses on increasing the risk of floods in the city of Saudi Arabia: A case study of the city of Hail using geographic information systems (GIS) and remote sensing (RS). *Arab. J. Geogr. Inf. Syst.* **2013**, *6*, 1–103.
29. El Adlouni, S.; Bobée, B. Hydrological Frequency Analysis Using HYFRAN-PLUS Software. 2015, pp. 1–71. Available online: https://www.scribd.com/document/307191717/ (accessed on 5 June 2022).
30. Environmental Modeling Research Laboratory of Brigham Young University. *Watershed Modeling System (WMS) v 8.1: Tutorials*; Environmental Modeling Research Laboratory of Brigham Young University: Provo, UT, USA, 2004.
31. Matthew, J.F. *Hydrologic Modeling System HEC-HMS, Quick Start Guide*; U.S Army Corps of Engineers, Hydrologic Engineering Center (HEC): St. Davis, CA, USA, 2013; Volume 4, 50p.
32. Feldman, A.D. *Hydrologic Modeling System HEC-HMS*; Hydrologic Engineering Center (HEC): St. Davis, CA, USA, 2008; 155p.
33. US Army Corps of Engineers (USACE). *River Analysis System HEC-RAS: Applications Guide*; Hydrologic Engineering Center (HEC): St. Davis, CA, USA, 2010.
34. Dragan, V.K.; Ivana, B.I.; Dejan, M.C.; Gordana, O.M. The initial analysis of the river Ibar temperature downstream of the lake gazivode. *Therm. Sci.* **2014**, *18*, 73–80.
35. Sunil, K.; Sayali, K.; Vrushali, B.; Akshada, W. Flood modeling of river godavari using hec-ras. *Int. J. Res. Eng. Technol.* **2014**, *3*, 81–87.
36. Raymond, D.; Soussou, S.; Seidou, K.; Issa, L.; Samo, D.; Mousse, L.; Didier, M. Calibration of HEC-RAS Model for One Dimensional Steady Flow Analysis - A Case of Senegal River Estuary Downstream Diama Dam. *Open J. Mod. Hydrol.* **2020**, *10*, 45–64.
37. Radmanesh, F.; Hemat, J.P.; Behnia, A.; Khond, A.; Mohamad, B.A. Calibration and assessment of HEC-1 model in Roodzard watershed. In Proceedings of the 17th International Conference of River Engineering, University of Shahid Chamran, Ahva, Iran, 26–28 February 2006; pp. 85–99.
38. Abdelkarim, A. *Hydrological and Hydraulic Modeling of Floods using Watershed Modeling System (WMS)*, 1st ed.; Al-Akiban Publishing House: Riyadh, Saudi Arabia, 2020; 484p.
39. Quan, V.D.; Kittiwet, K. An Assessment of Potential Climate Change Impacts on Flood Risk in Central Vietnam. *Eur. Sci. J.* **2015**, *1*, 667–681.
40. Ministry of Land, Infrastructure, Transport and Tourism (MLIT). *Manual for Economic Evaluation of Flood Control Investment (Draft)*; River Bureau, Ministry of Land, Infrastructure, Transport and Tourism: Tokyo, Japan, 2005; pp. 1–65. Available online: https://www.mlit.go.jp/river/kokusai/pdf/pdf06.pdf (accessed on 23 June 2022).
41. Hamed, Y. The hydrogeochemical characterization of groundwater in Gafsa-Sidi Boubaker region (Southwestern Tunisia). *Arab. J. Geosci.* **2013**, *6*, 697–710. [CrossRef]